Epitaxial $Pb(Zr_{0.53}Ti_{0.47})O_3/LaNiO_3$ heterostructures on single crystal substrates

Tao Yu, Yan-Feng Chen, Zhi-Guo Liu, Si-Bei Xiong, Li Sun, and Xiao-Yuan Chen
National Laboratory of Solid State Microstructures, Nanjing University, Nanjing 210093, People's Republic of China and Center for Advanced Studies in Science and Technology of Microstructures, Nanjing 210093, People's Republic of China

Lian-Je Shi
Department of Materials Science and Engineering, Nanjing University of Science and Technology, Nanjing 210014, People's Republic of China

Nai-Ben Ming[a)]
CCAST (World Laboratory), P.O. Box 8730, Beijing 100080, People's Republic of China and National Laboratory of Solid State Microstructures, Nanjing University, Nanjing 210093, People's Republic of China

(Received 19 February 1996; accepted for publication 24 July 1996)

Epitaxial near-stoichiometric ferroelectric $Pb(Zr_{0.53}Ti_{0.47})O_3$ thin films were fabricated on epitaxial metallic $LaNiO_3$ electrodes deposited on (001) $SrTiO_3$ and (001) $LaAlO_3$ single crystal substrates by pulsed laser ablation. The $P-E$ hysteresis loop of PZT in the trilayer of Ag/PZT/LNO/STO was measured using the Sawyer–Tower circuit. The remnant polarization P_r and coercive field E_c at room temperature were 30 $\mu C/cm^2$ and 69.3 kV/cm (peak-to-peak voltage=30 V, 50 Hz), respectively. © *1996 American Institute of Physics.* [S0003-6951(96)04140-X]

It is important to fabricate high quality ferroelectric thin films on the proper electrode materials primarily because of their potential use as high speed nonvolatile ferroelectric random access memories (NVFRAMs).[1] As favorable memory materials, the $PbZr_xTi_{1-x}O_3$ (PZT) class of perovskites and its derivatives have been successfully fabricated on some conductive oxide electrodes, such as $YBa_2Cu_3O_{7-x}$, $Bi_2Sr_2Ca_{n-1}Cu_nO_x$ $(n=1,2)$, $La_{0.5}Sr_{0.5}CoO_3$, $SrRuO_3$, $La_{2-x}Sr_xCuO_4$, RuO_2, and IrO_2.[2–9] These conductive oxide electrodes yield ferroelectric memories with better fatigue properties compared to the conventionally used platinum electrodes.[6,7]

The ternary compound $LaNiO_3$ (LNO) has a perovskite structure with a pseudocubic lattice parameter $a=3.84$ Å .[10] It has been reported that polycrystalline LNO without any doping is a Pauli paramagnetic material and an n-type metallic oxide (the electronic density $n=1.7\times10^{22}$ cm^{-3}).[11,12] Rajeev *et al.* studied the resistivity (ρ) of LNO from $T=0.4$ to 300 K and reported that the resistivity of LNO varied linearly as T with $(1/\rho)d\rho/dT=3.4\times10^{-3}$ K^{-1} ($\rho_{300\,K}=1.7$ mΩcm).[12] Satyalakshmi *et al.* first reported on epitaxial metallic LNO thin films on single crystals.[13] Since LNO has a good electrical conductive property and its structure is compatible with PZT class ferroelectric materials, it is a favorable candidate as an electrode for epitaxy of ferroelectric thin films.

The texture $Bi_2VO_{5.5}$ ferroelectric thin film was grown on LNO electrodes by Parasad *et al.*[14] Recently, the successful preparation of (100) and (001) textured PZT films on LNO-coated Si substrates by the sol-gel method was reported.[15] However, epitaxial PZT thin films on LNO electrodes have not been reported to our knowledge. In this letter, we first report on the fabrication and structure of epitaxial $Pb(Zr_{0.53}Ti_{0.47})O_3/LaNiO_3$ heterostructures on (001) $SrTiO_3$ and (001) $LaAlO_3$ single crystal substrates without a buffer layer. The ferroelectric property of epitaxial PZT thin films was characterized by $P-E$ hysteresis loop measurement.

The PZT/LNO heterostructures were fabricated by pulsed laser ablation (PLA) in our work. The PLA processes were performed by using Lambda Physik LPX205i KrF eximer laser system with 248 nm radiation in wavelength, 30 ns in pulse width, and 5 Hz in pulse frequency. In our experiment, the average laser pulse energy density was 200 mJ/mm.[2] The PZT and LNO targets used in this work were prepared by the standard sintering method. The nominal composition of PZT is Pb:Zr:Ti=1:0.53:0.47. The substrates were (001) $SrTiO_3$ (STO) and (001) $LaAlO_3$ (LAO) single crystals. LNO films were fabricated at 700 °C in 30 Pa oxygen partial pressure for 30 min. After deposition, the films were kept in 0.2 atm oxygen pressure for 30 min and then cooled to room temperature at a rate of about 10 °C/min. The typical LNO thickness was about 300 nm. A portion of the film was masked by aluminum foil. The deposition of PZT was then carried out under the same conditions as that of LNO for 20 min. The thickness of the PZT film was typically about 200 nm.

The chemical composition of PZT thin films was analyzed by the electron probe (EP) technique using a JAX-8800M electron probe microanalyzer. During EP analysis, the acceleration voltage was 15 kV and the probe diameter was 1 μm. Ten points were chosen to analyze on the PZT/LNO/LAO. The result showed that the Zr:Ti ratio in the PZT thin film was 0.51:0.49. In our experiment, the composition of the PZT target (Zr:Ti=0.53:0.47) was at the boundary between tetragonal and rhombohedral PZT. The composition of PZT films would be affected by the growth conditions such as the laser pulse energy density and oxygen partial pressure during PLA, but generally they were not exactly stoichiometric to that of the targets. If Zr:Ti>0.53:0.47, the

[a)]Electronic mail: naiben@bepc2.ihep.ac.cn

 0003-6951/96/69(14)/2092/3/$10.00

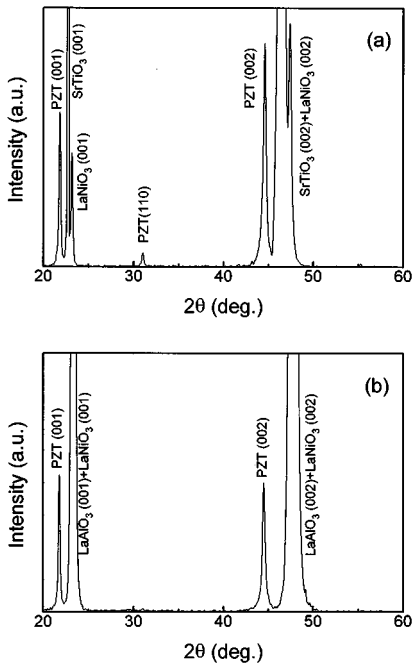

FIG. 1. The x-ray θ-2θ scan pattern of PZT thin films deposited (a) on LNO/STO and (b) on LNO/LAO substrates.

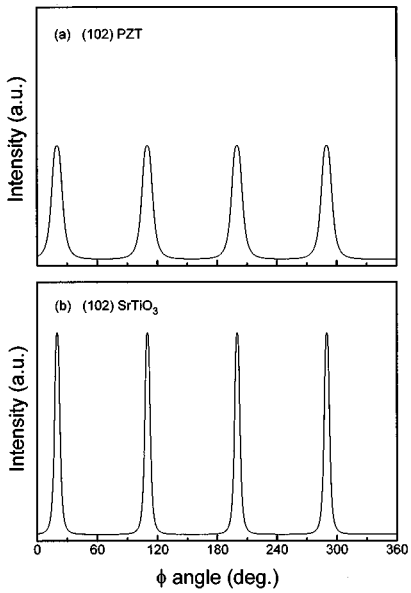

FIG. 2. The x-ray ϕ scan of (a) the (102) plane of the PZT thin film (FWHM=12°), and (b) the (102) plane of the STO single crystal substrate (FWHM=6°).

PZT thin film structure was rhombohedral. Otherwise, if Zr:Ti<0.53:0.47, the PZT thin film structure was tetragonal. The EP analysis result indicated that the PZT thin films were tetragonal in structure in our experiment.

The structures of PZT/LNO/STO and PZT/LNO/LAO were then characterized by x-ray θ–2θ scan using Cu K_α radiation on a Rigaku diffractometer. Figure 1 is the x-ray θ–2θ scan pattern of the PZT thin film deposited on LNO/STO and on LNO/LAO. In Figs. 1(a) and 1(b), only the (001) and (002) peaks of PZT and LNO thin films can be recognized. The weak peak at 31° in Fig. 1(a) is the x-ray diffraction of (110) PZT. It might come from the PZT droplets ($\sim$0.2 μm) on the thin film surface. The x-ray ϕ scan was carried out on LNO/STO and LNO/LAO; the results indicated that the LNO films were epitaxially grown on STO and LAO substrates.[16] Figure 1 revealed that the PZT films were highly *c*-axis oriented or epitaxially grown on the epitaxial LNO electrodes.

X-ray ϕ scan was carried out to confirm the epitaxial structures of PZT film on epitaxial LNO electrodes. In the x-ray ϕ scan measurement of PZT/LNO/STO, the (102) plane of PZT thin film and the (102) plane of the STO substrate were selected. When ψ, the tilt angle of the surface normal of the PZT/LNO/STO sample, was 26.57° and 2θ was fixed at 50.22°, the (102) plane ϕ scan result of the PZT film was obtained by rotating the sample 0°–360° around the surface normal. This result is plotted in Fig. 2(a). Then 2θ was fixed at 52.34°. The (102) plane ϕ scan result of the STO single crystal substrate could also be obtained by rotating the sample 0°–360° around the surface normal. This result is plotted in Fig. 2(b). In Fig. 2(a), four equally spaced peaks separated by 90° can be observed. The full width at half-maximum (FWHM) of each peak is 12°. This indicated that the surface normal (i.e., *c* axis of PZT thin film) is the fourfold symmetric axis of the PZT film. The peaks in Fig. 2(a) have no shift with respect to the peaks of the STO substrate (FWHM=6°) in Fig. 2(b). The ϕ scans displayed very wide peaks (for STO such scans give typically 0.5°–1.0° FWHM). The wide FWHM may come from the x-ray beam divergency in our measurement. The results should improve if the high quality x-ray beam were used. Comparing Figs. 2(a) and 2(b), we could conclude that the in-plane lattice vectors of the PZT film are aligned with that of the STO substrate. X-ray ϕ scan results confirmed that the PZT film was epitaxially grown on epitaxial LNO/STO, i.e., (001)PZT//(001)LNO//(001)STO, (010)PZT//(010)LNO//(010)STO and (100)PZT//(100)LNO//(100)STO. The epitaxial growth of the PZT/LNO heterostructure on the LAO substrate was also confirmed by x-ray ϕ scan.

We investigated the crystalline quality of the same PZT/LNO heterostructure on (001) STO or (001) LAO by Rutherford backscattering (RBS) spectroscopy along aligned $\langle 001 \rangle$ and random directions using 2 MeV He^+ ions. Figure 3 shows aligned and random spectra for the PZT/LNO bi-

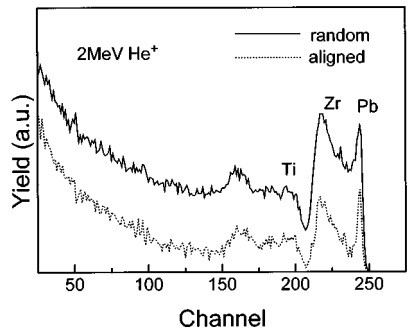

FIG. 3. Rutherford backscattering spectrum showing energe vs intensity for both channeling and random 2 MeV He^+ ions backscattered from a PZT/LNO heterostructure on the (001) LAO substrate; χ_{min} is 12.8%.

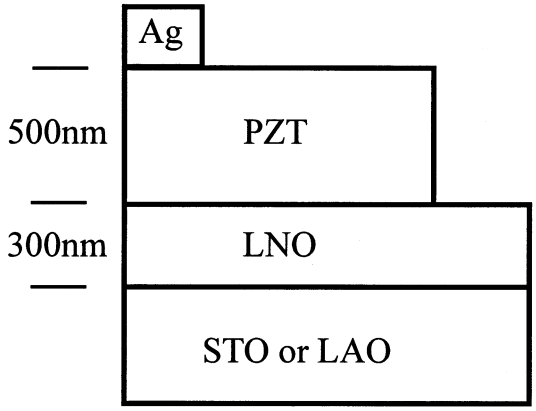

(a)

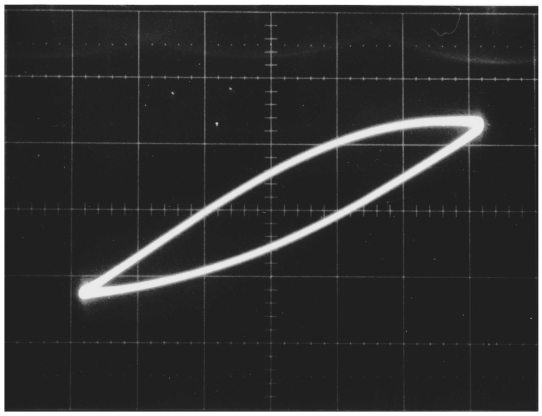

(b)

FIG. 4. (a) A schematic illustration of the setup used to test the ferroelectric properties of the heterostructures, and (b) the P–E hysteresis loop of the epitaxial PZT thin film in Ag/PZT/LNO/STO, $P_r = 30\ \mu\text{C/cm}^2$ and $E_c = 69.3$ kV/cm (peak-to-peak voltage=30 V, 50 Hz).

layer structure on the (001) LAO substrate. The ratio ($\chi_{\min}$) of the backscattered yield for the PZT/LNO heterostructure along $\langle 001 \rangle$ to that in random direction is 12.8%. This result indicates that the PZT/LNO heterostructure had better crystalline quality. There is strong dechanneling in the PZT/LNO heterostructure, particularly near the interface of PZT and LNO, that may contribute to the nonideal $\chi_{\min}$. This explanation has been suggested by Fork *et al.*[17] Another reason for the high ratio of the backscattered yield was that the direction of ion channeling was not positioned exactly at the $\langle 001 \rangle$ axis due to the limitation of the equipment we used. A detailed explanation can be found in our previous report.[18] With the sample positioned exactly, the result should be improved. Since the composition and structure of PZT/LNO were complex, the thickness of PZT and LNO thin films in the heterostructure and the Pb:Zr:Ti ratio were difficult to calculate from the RBS spectrum.

The ferroelectric behavior of epitaxial PZT thin films in the PZT/LNO/STO and PZT/LNO/LAO heterostructures was demonstrated by the P–E hysteresis loop measurement by using a Sawyer–Tower circuit. In this experiment, a thin layer of Ag with an area of 1.0 mm^2, deposited by the vacuum evaporation method was used as the top electrode. In this case, the remnant polarization (P_r) as well as the coercive field (E_c) dependence very much on the maximum voltage used; it meant that the PZT film was probably leaky. So we remeasured the P–E loops on thicker PZT films (thickness of 500 nm) and got satisfactory results. Figure 4(a) is a schematic illustration of the setup used to test the ferroelectric property of the PZT in heterostructures; Fig. 4(b) is the P–E hysteresis loop of the PZT thin film in the Ag/PZT/LNO/STO heterostructures. The remnant polarization (P_r) and coercive field (E_c) measured in our specimen at room temperature was 30 μ C/cm^2 and 69.3 kV/cm (peak-to-peak voltage=30 V, 50 Hz), respectively. The hysteresis loop in Fig. 4(b) was asymmetric; this meant that there was probably an interface between the ferroelectric thin film and the electrode.

The authors would like to thank Professor Wen-Lan Zhang for the help in electron probe analysis and Dr. Xian-Rong Huang for his helpful discussion. The project was supported by the 863 National High Technology Program and the National Natural Science Foundation of the People's Republic of China.

[1] J. F. Scott and C. A. Paz de Araujo, Science **246**, 1400 (1989).
[2] R. Ramesh, A. Inam, W. K. Chan, B. Wilkens, K. Mayers, R. Remsching, D. L. Hart, and J. M. Tarascon, Science **252**, 944 (1991).
[3] R. Ramesh, A. Inam, W. K. Chan, F. Tillerot B. Wilkens, C. C. Chang, T. Sands, J. M. Tarascon, and V. G. Keramidas, Appl. Phys. Lett. **59**, 3542 (1991).
[4] C. E. Eom, R. B. Van Dover, J. M. Phillps, D. J. Werder, J. H. Marshall, C. H. Chen, R. J. Cava, and R. M. Fleming, Appl. Phys. Lett. **63**, 2570 (1993).
[5] Y. Watanable, M. Tanamura, Y. Matsumoto, H. Asami, and A. Kato, Appl. Phys. Lett. **66**, 299 (1995).
[6] R. Ramesh, W. K. Chan, B. Wilkens, H. Gilchrist, T. Sands, J. M. Tarascon, V. G. Keramidas, D. K. Fork, J. J. Lee, and A. Safari, Appl. Phys. Lett. **61**, 1537 (1992).
[7] R. Ramesh, H. Gilchrist, T. Sands, V. G. Keramidas, R. Haakenaasen, and D. K. Fork, Appl. Phys. Lett. **63**, 592 (1993).
[8] J. T. Cheung, P. E. D. Morgan, and R. Neurgaonkar, Proceedings of the 4th International Synmposium Integrated Ferroelectrics, Colorado Springs, Colorado, 1992, p. 518.
[9] T. Nakamura, Y. Nakao, A. Kamisawa, and H. Takasu, Jpn. J. Appl. Phys. **33**, 5207 (1994).
[10] A. Wold, B. Post, and E. Banks, J. Am. Ceram. Soc. **79**, 4911 (1957).
[11] P. Ganguly, N. Y. Vasanthacharya, C. N. R. Rao, and P. P. Edwards, J. Solid State Chem. **54**, 400 (1984).
[12] K. P. Rajeev, G. V. Shivashankar, and A. K. Raychaudhuri, Solid State Commun. **79**, 591 (1991).
[13] K. M. Satyalakshmi, R. M. Mallya, K. V. Ramanathan, X. D. Wu, B. Brainard, D. C. Gautier, N. Y. Vasanthacharya, and M. S. Hedge, Appl. Phys. Lett. **62**, 1233 (1993).
[14] K. V. R. Prasad, K. B. R. Varma, A. R. Raju, K. M. Satyalakshmi, R. M. Mallya, and M. S. Hedge, Appl. Phys. Lett. **63**, 1898 (1993).
[15] C. C. Yhang, M. S. Chen, T. J. Hong, C. M. Wu, J. M. Wu, and T. B. Wu, Appl. Phys. Lett. **66**, 2643 (1995).
[16] T. Yu, Y. F. Chen, Z. G. Liu, X. Y. Chen, L. Sun, N. B. Ming, and L. J. Shi, Mater. Lett. **26**, 73 (1996).
[17] D. K. Fork, D. B. Fenner, G. A. N. Connell, J. M. Pillips, and T. H. Geballe, Appl. Phys. Lett. **57**, 1137 (1990).
[18] Y. F. Chen, L. Sun, T. Yu, J. X. Chen, N. B. Ming, D. S. Ding, and L. W. Wang, Appl. Phys. Lett. **67**, 3503 (1995).